IEEE Access
Multidisciplinary ⋮ Rapid Review ⋮ Open Access Journal

Received September 28, 2018, accepted October 11, 2018, date of publication October 15, 2018, date of current version November 14, 2018.

Digital Object Identifier 10.1109/ACCESS.2018.2876236

Decision Theory Criteria for the Planning of Distributed Energy Storage Systems in the Presence of Uncertainties

AMEDEO ANDREOTTI[1], (Senior Member, IEEE), GUIDO CARPINELLI[1], (Member, IEEE), FABIO MOTTOLA[1], (Senior Member, IEEE), DANIELA PROTO[1], (Senior Member, IEEE), AND ANGELA RUSSO[2], (Senior Member, IEEE)

[1]Department of Electrical Engineering and Information Technology, University of Naples Federico II, 80125 Naples, Italy
[2]Energy Department "Galileo Ferraris", Politecnico di Torino, 10129 Turin, Italy

Corresponding author: Fabio Mottola (fmottola@unina.it)

ABSTRACT This paper deals with the use of distributed energy storage systems in microgrids, and proposes a planning method which accounts for the uncertainties of load and distributed generation. Objectives of the planning method are the reduction of the energy costs, while providing the supply of ancillary services as a technical support to the network. The energy costs are evaluated considering a hourly varying pricing scheme and optimizing the storage systems charging/discharging stages. The technical support is devoted to the restraint of bus voltage amplitudes, and of network components' currents/powers within admissible ranges. The input data uncertainties are managed through three decision theory criteria (i.e., the minimization of expected costs; an approach based on the weighted regret felt by the design engineer; and a stability area criterion), which allow considering the multiple design alternatives and futures (i.e., possible values of uncertain input data) in an accurate and feasible way. The design alternatives refer to the size and location of the distributed storage systems, while each future is associated with a different level of load demand and power production of distributed generation over the whole planning period. The results of numerical applications are reported and discussed with reference to a Cigré test network.

INDEX TERMS Microgrids, energy storage, optimal planning, decision theory.

NOMENCLATURE

$A_{opt,ec}$	Best alternative associated with the lowest value of the expected total costs
$A_{opt,r}$	Best alternative associated with the minimum among the maximum weighted regrets
A_p	pth alternative
$B_{i,j}$	(i,j)-term of the system's susceptance matrix
C_{inst}	Cost sustained for the installation and replacement of the EESS
C_{op}	Cost sustained to purchase energy from the upstream grid
C_T	Total cost
$C_T^{opt}\left(F_q\right)$	Minimum total cost for the future F_q
$EC_T\left(A_p\right)$	Expected total cost associated with all the futures for the alternative A_p
DG	Distributed generation
DM	Decision Maker
DoD	Depth of Discharge
$E_{b,i}^{rtd}$	Energy capacity of the ith EESS
$E_{EESS_i}^{size}$	Size of the ith EESS
EESS	Electrical energy storage systems
F_q	qth future
$G_{i,j}$	(i,j)-term of the system's conductance matrix
$I_{l,k_{(y,d)}}$	Current flowing through the lth line during the kth time interval of the dth typical day of the year y
$I_{l,max}$	Ampacity of the lth line
IC_{EESS}	Capacity unitary cost of the EESS
L_b	Battery's lifetime
$N_{cycles}(\text{DoD})$	Total number of cycles related to specified DoD of the battery
$N_{y,d}$	Number of days represented by the dth typical day in the year y

OPF	Optimal power flow
$P_{1,k_{(y,d)}}$	Power imported from the upstream network during the kth time interval of the dth typical day of the year y
$P_{b,i,k_{(y,d)}}$	Active power of the ith EESS during the kth time interval of the dth typical day of the year y
$P^{rtd}_{b,i}$	Rated power of the ith EESS
$P_{dg,i,k_{(y,d)}}$	Active power of the ith DG unit during the time interval k of the day d, year y
$P_{i,k_{(y,d)}}$	Net active power injected at the bus i during the kth time interval of the dth typical day of the year y
$P_{ld,i,k_{(y,d)}}$	Active power requested by the load at the bus i during the kth time interval of the dth typical day of the year y
P_{max}	Admissible maximum value of the power imported by the μG
$Pr_{k_{(y,d)}}$	Hourly energy price during the kth time interval of the dth typical day of the year y
$P_{v,k_{(y,d)}}$	Active power flowing through the vth transformer during the kth time interval of the dth typical day of the year y
$Q_{b,i,k_{(y,d)}}$	Reactive power of the ith EESS during the time interval k of the day d, year y
$Q_{dg,i,k_{(y,d)}}$	Reactive power of the ith DG unit during the time interval k of the day d, year y
$Q_{i,k_{(y,d)}}$	Net reactive power injected at the bus i during the kth time interval of the dth typical day of the year y
$Q_{ld,i,k_{(y,d)}}$	Reactive power requested by the load at the bus i during the kth time interval of the dth typical day of the year y
$Q_{v,k_{(y,d)}}$	Reactive power flowing through the vth transformer during the kth time interval of the dth typical day of the year y
$R\left(A_p, F_q\right)$	Regret felt for having chosen the design alternative A_p when the future F_q occurred
$R_w\left(A_p, F_q\right)$	Weighted regret
R^{max}_w	Maximum weighted regret
RC_{EESS}	Replacement unitary cost of the EESS
SOC	State of charge
$S^{rtd}_{DESS,i}$	Rated power of the converter of the ith EESS
$S^{rtd}_{DG,i}$	Rated power of the converter of the ith DG unit
$S^{rtd}_{tr,v}$	Rated power of the vth transformer
$V_{j,k_{(y,d)}}$	Magnitude of the voltage at the jth bus during the kth time interval of the dth typical day of the year y
V_{min}	Minimum value that the bus voltage magnitude can assume at the generic bus i
V_{max}	Maximum value that the bus voltage magnitude can assume at the generic bus i
V_{spec}	Specified value of the voltage magnitude at the slack bus
a	Discount rate
$e_{b,i_{(y,d)}}$	Sum of the energy effectively discharged in all of the intervals of the day d, year y
f_{obj}	Objective function of the OPF
n	Number of μG buses
na	Number of alternatives
nb	Number of EESSs
$n_{cycles,d}$	Number of daily charging/discharging cycles of the battery
nd_y	Number of typical days of each year y
nf	Number of futures
nt	Number of time intervals in which each day is divided
ny	Number of years of the planning period
Δt	Duration of each time interval
$\Omega_{ch_{(y,d)}}$	Set of time intervals of the day d of the year y in which the EESS can only be charged
$\Omega'_{ch_{(y,d)}}$	Sorted set of time intervals of $\Omega_{ch_{(y,d)}}$
$\Omega_{dch_{(y,d)}}$	Set of time intervals of the day d of the year y in which the EESS can only be discharged
$\Omega'_{dch_{(y,d)}}$	Sorted set of time intervals of $\Omega_{dch_{(y,d)}}$
Ω_{DESS}	Set of buses where EESSs are connected
Ω_{DG}	Set of buses where DG units are connected
Ω_l	Set of the line of the μG
Ω_{tr}	Set of buses where transformers are connected
ϕ_γ	γth inequality constraint of the OPF
ψ_ν	ν th equality constraint of the OPF
δ	Maximum admissible DoD
$\delta_{i,k_{(y,d)}}$	Argument of the voltage at the jth bus during the kth time interval of the dth typical day of the year y
$\eta_{ch,i}$	Charging efficiency of the ith EESS
$\eta_{dch,i}$	Discharging efficiency of the ith EESS
μG	Microgrid
ω_q	Probability of occurrence of the qth future

I. INTRODUCTION

Thanks to their wide range of applications, electrical energy storage systems (EESSs) are becoming the key components in any practical development of microgrids (μGs), where loads and distributed generation (DG) units are clustered and connected to an upstream distribution network [1], [2]. EESSs can be exploited to pursue several objectives that range from load leveling to integration of renewable and intermittent sources. Objectives related to power quality can also be pursued, such as the voltage profiles and unbalances, that can be improved thanks to the storage's optimal control.

The significant contribution of EESSs is also in that they help achieve the participation of consumers in the system operation so enhancing effective operation of the power distribution system. This particular application is framed in the well-known demand response paradigm.

The most effective ways to incentivize demand response are the price-based programs [3], where the customers modify their energy requests according to the price variations during the day. In this context, the role of storage devices is essential since they are able to shift the load demand in compliance with the price variations [4]–[11]. While these contributions are apparent, it has to be noted that EESSs are expensive, and their optimal planning in μGs is crucial to minimize the total investment cost while meeting system requirements. Then, recent technical literature widely focused on the problem of the optimal siting and sizing of distributed storage devices in electrical networks [12]–[34]. The primary issue addressed in [12]–[34] aims to maximize the economic viability of the storage operation by minimizing the investment and operational costs while preserving the operation constraints of the electrical network. In [12] a method is proposed for allocating battery storage systems: the proposal is based on a cost-benefit analysis aimed at maximizing the profit of distribution companies by modifying the procurement of energy according to the electricity price variations. In [13] a method for the siting and sizing of both battery storage systems and micro-turbines is proposed which aims to reduce the costs sustained by the grid operator. In [14] the optimal siting and sizing of energy storage systems aims to reduce the costs sustained by the distribution network operator while accounting for the provision of ancillary services through a multi-objective approach. The planning tool proposed in [15] focuses on optimal allocation of battery storage systems in distribution networks and aims to decrease power fluctuations due to renewable energy sources, and to control frequency when contingencies occur in the interconnected transmission network. In the planning approach discussed in [16], battery storage systems are optimally sited and sized, with the aim of minimizing costs related to energy consumptions. With reference to island operation mode, a multi-objective optimal planning tool is proposed in [17] for the minimization of the amount of energy storage, power losses and expected energy not supplied. In [18] the planning method is proposed with reference to energy storage systems in unbalanced μGs, with the objective of reducing the costs sustained by the μG under time of use pricing while satisfying network's constraints. In [19], the proposed allocation method allows the storage systems to provide active and reactive support in view of reactive power/voltage regulation, losses reduction and cost minimization. The method proposed in [20] refers to the optimal allocation of energy storage systems, shunt capacitors and renewable generation units in active distribution networks aimed at minimizing the cost sustained by the network operator and the power losses. In [21] a method is proposed which optimizes the relationship between net income and storage capacity. In [22] an allocation method is proposed which incorporates network reconfiguration and performs the optimal power flow (OPF) by accounting for voltage deviation and lines' congestion. In the methodology presented in [23], which refers to the allocation of energy storage and renewable generation, the use of the storage is devoted to peak shaving and loss reduction, while the objective of the optimization is to maximize the economic benefits of both distribution system operator and renewable generation owner. In [24] optimal allocation of energy storage systems and DG in μGs is proposed aimed at minimizing the operation and investment costs of the μG. In [25], a method is proposed for the optimal allocation of EESSs in unbalanced distribution systems with the aim of the cost minimization. An approach is proposed in [26] for the optimal placement of energy storage devices aimed at improving the transient stability of the μG (in this regard, the economic issue is neglected). In [27], a method for the optimal planning of batteries to minimize the cost objective function is proposed in the case of large penetration of wind sources. In [28] the optimal planning of storage devices is performed through an optimization of costs and reliability in the presence of renewable generation and plug-in electric vehicles. A method for the optimal planning of storage systems used to mitigate voltage fluctuations in distribution networks is proposed in [29]. In [30] a cost-based method is proposed for the optimal planning of storages in power systems. A multi-objective approach is proposed in [31] to model the optimal planning of storage systems in active distribution systems. In [32] an optimization model is proposed for planning storage devices in power grids with intermittent wind generation. An optimal model is proposed in [33] for the planning of distributed storage systems coordinated with devices used for active/reactive support in distribution networks. Reference [34] provides a comprehensive overview on the methods proposed in the technical literature for the allocation of EESSs.

Optimal allocation models for EESSs are typically formulated as mixed, integer, non-linear optimization problems subject to equality and inequality constraints. The presence of the energy storage devices requires to solve multi-period optimization problems: the active power of the storage device depends, at any time, on the actual state of charge (SOC), thus implying that power and SOC of the batteries are to be optimized throughout all time intervals of the optimization horizon simultaneously. Further complexities derive from other constraints imposed on the SOC of the battery, such as the number of charging/discharging cycles, which have to be properly limited to prolong battery lifetime. Integration of storage devices in modern distribution grids also implies the control of reactive power, in order to better coordinate distributed resources and provide technical support to the network.

Taking into account all of the above aspects makes the solution of the planning problem very difficult using any mathematical approaches, so making the rigorous solutions impracticable from the computational point of view. This is even more critical in realistic applications, where the problem is further complicated by the presence of a large number of network buses and, in this case, probabilistic approaches are used to face with the unavoidable uncertainties affecting the forecast of load and generation. Indeed, randomness of load and generation powers have a significant impact on the evaluation of the storage system's sizing cost. Uncertainties related to energy prices, discount rates and those related to the technological features of the storage systems (i.e. lifetime duration, roundtrip efficiency and capital, operation, maintenance and replacement unit costs) have influence too. References [35] and [36] analyze the above uncertainties and show that they have different impacts on the storage system's probabilistic sizing.

Many efforts have been done in the literature in order to find algorithms able to manage the complexities affecting the problem of the optimal allocation and sizing of storage devices. For instance, the following algorithms have been recently used: fuzzy particle swarm optimization [12], alternating direction method of multipliers [14], complex-valued neural networks [15], GA based approaches [18]–[20], [25], [29] inherent structure theory of networks and loading constraints criterion [18], sequential quadratic programming [18]–[20], greedy algorithm [21], Benders decomposition [22], [30], grey wolf [23], hybrid tabu search/particle swarm optimization algorithm [27], [28], optimal affine power flow approach [29], differential evolution and particle swarm optimization [31], parallel Branch and Bound algorithm [32], mixed-integer second-order-cone programming [33] and simultaneous perturbation stochastic approximation [25].

To include uncertainties within the planning problem, a two-stage approach is used in [13], a probabilistic power flow based on the point estimate method is used in [17], [27], [28], and [32], specific scenarios are derived from various probability models to account for variations and uncertainties of the inputs in [14], [21]–[25], [30], and [31].

In this paper, the complexity involved in the planning of distributed EESSs in μGs under uncertainties is faced by using a probabilistic approach based on a stepwise procedure, i.e., (i) a limited number of selected siting and sizing alternatives for the EESSs and of futures (i.e., possible values of uncertain input data) are chosen; (ii) a probability is assigned for each future; (iii) the total costs (investment and operation costs) are calculated for each alternative and future (that is, for each scenario) applying a minimum cost control strategy of the μG; and (iv) Decision Theory is used to obtain the best size and site for the EESSs, taking into account the total costs and future probabilities. In particular, three approaches provided by Decision Theory have been considered which are based on the (1) minimization of expected total costs; (2) minimization of the regret felt by the engineer who is sizing the EESSs (hereafter referred to as the ''Decision Maker'', DM); (3) evaluation of the solutions for which both the decision criteria (1) and (2) provide the same optimal solution (stability areas). These approaches have been used extensively and successfully to solve several important planning problems associated with power systems [37]–[41].

Regarding uncertainties, from a theoretical point of view, all the aforementioned random variables (energy price, load and generation powers, etc.) could be considered in the proposed procedure by a proper definition of the futures. Without loss of generality, to avoid verbose presentation of the results, uncertainties considered in the numerical application of this paper refer only to load and generation powers.

Moreover, in order to significantly limit the computational burden, in this paper a simplified but effective minimum cost control strategy is applied to the μG. More specifically, the daily profiles of the EESSs' active power are analytically derived, first. This is done, on the basis of the hourly value of the energy price and on the constraints related to the EESS. Then, having the EESS's active power profiles as inputs, OPFs are separately performed at each of the time intervals in which the day is divided, in order to control the reactive power of the energy resources (i.e., EESSs and DG units) with the aim of minimizing the imported power from the upstream grid while satisfying technical constraints on the μG. The combination of these two steps allows obtaining the minimization of the total costs for each scenario, while preserving the computational burden of the proposed solution method, since the multi-temporal constraints on the EESSs are imposed only at the first step.

The main contributions of the probabilistic approach proposed in this paper are:

- application of a planning method able to catch the potential of the use of EESSs in μGs in terms of both technical and economic advantages;
- proposal of a new approach for solving the EESSs' allocation (siting and sizing) problem based on the proper integration of a minimum cost strategy into a Decision Theory framework. With such an approach, the economic and technical aspects of the EESSs' allocation and uncertainties affecting loads and generation are accounted for in a feasible way;
- application of a minimum cost strategy which allows controlling the EESSs' active and reactive powers and DG units' reactive power in order to reduce the cost for the power imported by the μG from the upstream distribution network. The optimization is performed satisfying technical and operation constraints of the μG and its resources;
- use of three Decision Theory-based approaches to obtain the best sizing/siting alternative considering the various uncertainties involved in the allocation framework.

The remainder of the paper is organized as follows. The planning method, which is formulated in terms of optimal allocation problem under uncertainties, is introduced in Section II, along with the proposed solution procedure. In Section III the determination of the total costs related to the μG operation and to the inclusion of EESSs is detailed along with the minimum cost strategy adopted for the μG operation. The Decision Theory criteria and the way they are used in the proposed approach are discussed in Section IV. The results of a numerical application on a Cigré test network are reported and discussed in Section V. Conclusions are drawn in the last Section.

II. THE OPTIMAL ALLOCATION PROBLEM

The proposed approach for the optimal siting and sizing of EESSs in μGs under uncertainties is based on the application

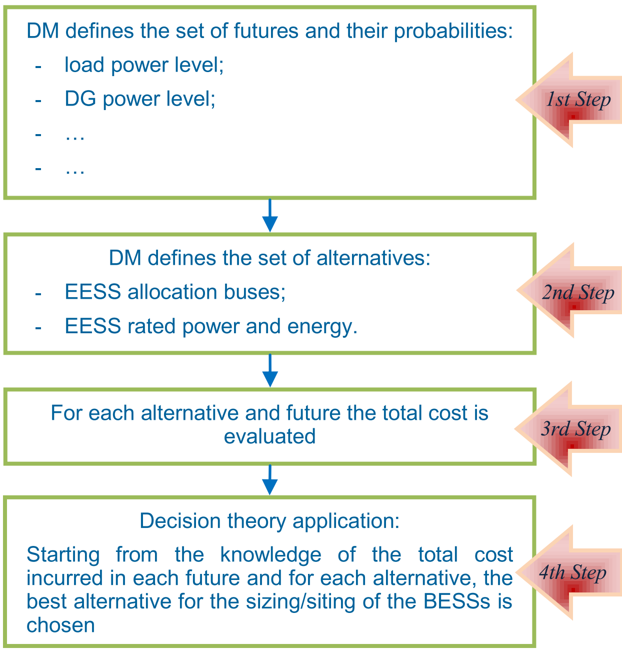

FIGURE 1. Flow chart of the procedure.

of the Decision Theory and is summarized in the flow chart of Fig. 1.

A four-step procedure is applied:

1. A set of possible futures is specified, and each future is characterized by a probability assigned by the DM. In this paper, each future is associated with a different level of load demand and DG power production.

2. Several possible EESSs design alternatives are specified. Each design alternative is based on the EESSs location and size (this last is expressed in terms of rated power and energy capacity).

3. Total costs are calculated for each future specified in the first step and for each alternative specified in the second step. Since in a μG the total cost depends on the way the EESSs and the other resources (e.g., DG units) are operated, a proper optimization tool for the optimal operation of the EESSs and of the other resources is applied. The tool allows controlling the EESSs' active and reactive power and DG units' reactive power in order to reduce the cost sustained for the power imported by the μG from the upstream distribution network. The optimization is performed while satisfying the technical and operation constraints of the μG and of its resources.

4. The Decision Theory is applied to choose, among the alternatives of Step 2, the best EESS sizing/siting solution by considering the futures with their probabilities, as specified in Step 1. The applied Decision Theory approaches are the minimization of the expected cost, the min-max weighted regret, and the maximization of the stability areas' criteria.

It should be noted that the DM selects alternatives and futures of Steps 1 and 2 and assigns the future probabilities.

In order to estimate the probabilities to be assigned when the future uncertainties are modeled probabilistically there are three possible approaches that are typically used:

- The first approach is based completely on the observed information.
- The second approach is based completely on the subjective judgment of the DM.
- The third approach is a mix of the above two approaches, and it combines the DM's judgmental information with the observed information.

More details on the three approaches can be found in [37]. In this paper, we used the second approach (subjective judgment of the DM [37]–[41]). It may seem unsound to assign values of probabilities with little or no empirical information, but it is well known that, surprisingly, positive results can be obtained when the DM has a good understanding of the nature of the uncertainties relevant to the problem and uses this understanding to assign probabilities in a subjective manner [37]–[41].

In the next Sections, we show the details of the total cost evaluation of Step 3 and the decision theory criteria of Step 4.

III. TOTAL COST EVALUATION

In this section, the procedure to evaluate the total cost related to the inclusion of EESSs in the μG is detailed referring to an assigned design alternative and an assigned future. This cost depends on the cost for the installation of EESSs and on the cost for the operation of the network with reference to a specified planning period:

$$C_T\left(A_p, F_q\right) = C_{inst}\left(A_p\right) + C_{op}\left(A_p, F_q\right) \qquad p = 1, \ldots, na, \quad q = 1, \ldots, nf \tag{1}$$

where A_p is the pth alternative, F_q is the qth future, $C_T\left(A_p, F_q\right)$ is the total cost, $C_{inst}\left(A_p\right)$ is the cost sustained for the installation and replacement of the EESSs, and $C_{op}\left(A_p, F_q\right)$ refers to the cost sustained to purchase energy from the upstream grid.

The installation cost depends on rated power and energy capacity of the battery whose unitary cost values depend on the specific battery technology. Furthermore, in the case replacement of the battery is required, also the corresponding cost item must be considered. The installation cost is then given by:

$$C_{inst}(A_p) = \sum_{i=1}^{nb}\left[(IC_{EESS} + r_i RC_{EESS})E^{size}_{EESS_i}\right] \quad p = 1, \ldots, na \tag{2}$$

where IC_{EESS} is the capacity unitary cost, RC_{EESS} is the replacement unitary cost which is included to take into account the battery's degradation cost [42], [43], nb is the number of EESSs, $E^{size}_{EESS_i}$ is the size of the ith EESS and r_i assumes value 1 if replacement of the ith battery is needed, 0 otherwise. The value of r_i is obtained by comparing the battery's lifetime duration (in years) with the planning period. The battery's lifetime L_b (in years), indeed, can be evaluated as:

$$L_b = \frac{N_{cycles}(DoD)}{365 n_{cycles,d}} \tag{3}$$

with $N_{cycles}(DoD)$ the total number of cycles related to specified depth of discharge (DoD) and ambient temperature, $n_{cycles,d}$ the number of daily charging/discharging cycles. Thus, when L_b exceeds the planning period the replacement is needed and r_i assumes the value 1. Eq. (2) refers to the possibility of one replacement; the extension to the case of more than one replacement is trivial. Note also that IC_{EESS} and RC_{EESS} are related to the capacity and the rated power which are linked to each other through the rated discharge time. In (2), maintenance costs could be included as percentage of the installation cost [44].

In order to evaluate operation cost, each year of the planning period is divided in typical days, which are characterized by specified load power demand, generation power production, energy price and their yearly growth. The characteristics of the typical days depend on the considered future. The operation cost is then given by:

$$C_{op}\left(A_p, F_q\right) = \sum_{y=1}^{ny} \frac{1}{(1+a)^{y-1}} \times \sum_{d=1}^{nd_y} N_{y,d} \left[\sum_{k=1}^{nt} \left(P_{1,k_{(y,d)}} \Delta t\right) Pr_{k_{(y,d)}}\right] \quad (4)$$

where ny is the number of years of the planning period, nd_y is the number of typical days of each year y, $N_{y,d}$ is the number of days represented by the dth typical day in the year y, nt is the number of time intervals in which each day is divided, Δt is the duration of each time interval, a is the discount rate and $P_{1,k_{(y,d)}}$ is the power imported from the upstream network during the kth time interval of the dth typical day of the year y. This last term is subject to a specific hourly energy price which is $Pr_{k_{(y,d)}}$.

The power imported from the upstream grid, i.e. the term $P_{1,k_{(y,d)}}$ in (4), which depends on both future and alternative, is evaluated as output of the minimum cost strategy that is based on a two-step procedure:

A. the optimal active power profiles of the EESSs are first determined according to both hourly energy prices and EESSs constraints;
B. nt OPFs are performed on the μG with the aim of minimizing the power imported from the upstream grid while satisfying the network technical constraints. Note that the active power profiles of the EESSs are those derived in the first step.

The first step aims at evaluating the daily active power profiles of the EESSs based on the costs' minimization. This is done by charging the battery during low price hours and discharging during the high price hours. At this step, constraints are imposed only on the rated power and energy capacity of the EESSs.

The OPF solved in the second step is performed for each time interval of the day. Inputs of the optimization are the specified values of loads' active and reactive powers and active powers of DG units and EESSs. Objective of the OPF is the minimization of the power imported from the upstream grid and, then, the network losses. The control of the reactive powers of DG units and EESSs in this step allows both the minimization of the objective function and the satisfaction of the technical constraints on the μG.

Both these steps are detailed in the following sub-sections.

A. OPTIMAL PROFILE OF THE EESS

In order to determine the optimal power profile of the EESS, the following procedure is proposed. The set of time intervals in which the EESS can be charged and discharged, respectively, is identified on the basis of the energy price values. More specifically, with reference to the day d of the year y, the time intervals in which the EESS can only be discharged ($\Omega_{dch_{(y,d)}}$) are those characterized by higher prices of the energy whereas the time intervals in which the EESS can only be charged ($\Omega_{ch_{(y,d)}}$) are those characterized by lower prices of the energy. These sets of time intervals are chosen so that only one charging/discharging cycle per day is allowed.

The time intervals in $\Omega_{dch_{(y,d)}}$ are sorted starting from that with the highest energy price up to that with the lowest energy price. For clarity purposes, hereinafter we will refer to this sorted set as $\Omega'_{dch_{(y,d)}}$. Once defined this priority order, the power profile of the battery is derived by imposing that the energy stored in the battery is discharged during the time intervals of highest prices, first, and then during the other intervals. At each time interval, the value of the power discharged by the battery is limited by the rated active power and the constraints on the SOC. Thus, with reference to the kth interval, when the rated capacity of the EESS is sufficient to discharge the battery at its rated power in all the preceding time intervals including the current kth interval (that is when $1/\eta_{dch,i}\left(kP_{b,i}^{rtd}\Delta t\right) \leq \delta E_{b,i}^{rtd}$), the power discharged is:

$$P_{b,i,k_{(y,d)}} = P_{b,i}^{rtd} \quad k \in \Omega'_{dch_{(y,d)}} \quad y = 1, \ldots, ny, \quad d = 1, \ldots, nd_y \quad (5)$$

where, with reference to the ith EESS, time interval k of the day d, year y, $P_{b,i,k_{(y,d)}}$ is the active power of the EESS, $P_{b,i}^{rtd}$ is the rated power of the EESS, $\eta_{dch,i}$ is its discharging efficiency, $E_{b,i}^{rtd}$ is the EESS energy capacity and δ is the maximum admissible depth of discharge. Note that δ is fixed once the battery technology and the number of daily charging/discharging cycles is known, on the basis of the desired lifetime duration. Otherwise, when the rated capacity of the EESS is not sufficient to discharge the battery at its rated power in all the preceding time intervals including the current kth interval (that is $1/\eta_{\mathrm{dch,i}}\left(kP_{b,i}^{rtd}\Delta t\right) > \delta E_{b,i}^{rtd}$) the power discharged is by the EESS is:

$$P_{b,i,k_{(y,d)}} = \begin{cases} \eta_{dch,i}\dfrac{1}{\Delta t}\left(\delta E_{b,i}^{rtd} - \frac{(k-1)}{\eta_{dch,i}}P_{b,i}^{rtd}\Delta t\right) & if\ \vartheta(k) \geq 0 \\ 0 & otherwise \end{cases} \quad (6)$$

with $k \in \Omega'_{dch_{(y,d)}}$, $y = 1, \ldots .ny$, $d = 1, \ldots nd_y$ and

$$\vartheta(k) = \delta E^{rtd}_{b,i} - \frac{(k-1)}{\eta_{dch,i}} P^{rtd}_{b,i} \Delta t$$

Note that if positive, $\vartheta(k)$ is the remaining energy to be discharged at the kth time interval.

The sum of the energy effectively discharged in the all of the intervals, $e_{b,i_{(y,d)}}$, is then given by:

$$e_{b,i_{(y,d)}} = \frac{1}{\eta_{dch,i}} \sum_{k \in \Omega_{dch_{(y,d)}}} P_{b,i,k_{(y,d)}} \Delta t \qquad y = 1, \ldots, ny, \quad d = 1, \ldots, nd_y \quad (7)$$

To evaluate the power absorbed by the EESS, the time intervals included in $\Omega_{ch_{(y,d)}}$ are sorted starting from that with the lowest energy price up to that with the highest energy price, obtaining the sorted set $\Omega'_{ch_{(y,d)}}$.

The power profile of the battery is derived by imposing that the energy is charged during time intervals of lowest prices, first, and then during the other intervals. At each time interval, the value of the power charged by the battery is limited by the rated active power and by the maximum energy that can be charged. This value must be equal to the energy effectively discharged, $e_{b,i_{(y,d)}}$, since the values of the energies charged and discharged during the day must be equal. Thus, when the energy charged in all the preceding time intervals including the current kth interval does not exceed $e_{b,i_{(y,d)}}$ (that is when $\eta_{ch,i}\left(kP^{rtd}_{b,i}\Delta t\right) \le e_{b,i_{(y,d)}}$, with $\eta_{ch,i}$ the charging efficiency of the EESS), the power charged by the EESS is equal to its rated value:

$$P_{b,i,k_{(y,d)}} = -P^{rtd}_{b,i} \quad k \in \Omega'_{ch_{(y,d)}} \qquad y = 1, \ldots, ny, d = 1, \ldots, nd_y \quad (8)$$

Otherwise, when $\eta_{ch,i}\left(kP^{rtd}_{b,i}\Delta t\right) > e_{b,i_{(y,d)}}$ the power charged is:

$$P_{b,i,k_{(y,d)}} = \begin{cases} \dfrac{-1}{\eta_{ch,i}\Delta t}\left(e_{b,i_{(y,d)}} - \eta_{ch,i}(k-1)P^{rtd}_{b,i}\Delta t\right) & if\ \vartheta'(k) \ge 0 \\ 0 & otherwise \end{cases} \quad (9)$$

with $k \in \Omega'_{ch_{(y,d)}}$, $y = 1, \ldots, ny$, $d = 1, \ldots, nd_y$ and

$$\vartheta'(k) = e_{b,i_{(y,d)}} - \eta_{ch,i}(k-1)P^{rtd}_{b,i}\Delta t$$

Note that, if positive, $\vartheta'(k)$ is the remaining energy to be charged at the kth time interval. The energy effectively charged in all of the intervals, $e'_{b,i_{(y,d)}}$, is then given by:

$$e'_{b,i_{(y,d)}} = -\eta_{ch,i} \sum_{k \in \Omega_{ch_{(y,d)}}} P_{b,i,k_{(y,d)}} \Delta t \qquad y = 1, \ldots, ny, d = 1, \ldots, nd_y \quad (10)$$

Once $e'_{b,i_{(y,d)}}$ is calculated, it must be verified that $e'_{b,i_{(y,d)}} = e_{b,i_{(y,d)}}$. In the case this condition does not occur, the discharging power must be recalculated by substituting $\delta E^{rtd}_{b,i}$ in (5)-(7) with $e'_{b,i_{(y,d)}}$.

B. OPTIMAL POWER FLOW

The OPF is formulated for each time interval k of the day d, year y, in terms of non linear constrained single objective minimization problem:

$$min\, f_{obj}(\boldsymbol{x}) \quad (11)$$
$$\psi_\nu(\boldsymbol{x}) = 0 \quad \nu = 1, \ldots, n_{eq} \quad (12)$$
$$\phi_\gamma(\boldsymbol{x}) \le 0 \quad \gamma = 1, \ldots, n_{ineq} \quad (13)$$

where f_{obj} is the objective function, ψ_ν and ϕ_k are the νth equality and γth inequality constrained functions, respectively. Vector $\boldsymbol{x}$ includes the optimization variables (f.i., the power imported from the upstream network and the reactive power of DG units and EESSs). The objective function to be minimized is the power provided to the μG by the upstream grid in the generic time interval:

$$f_{obj}(\boldsymbol{x}) = P_{1,k_{(y,d)}} \qquad k = 1, \ldots, nt, \quad y = 1, \ldots, ny, \ d = 1, \ldots, nd_y \quad (14)$$

It is worth nothing once again that the minimization of (14) allows minimizing the grid losses.

Equality constraints refer to the active and reactive power balances at each bus i of the μG:

$$P_{i,k_{(y,d)}} = V_{i,k_{(y,d)}} \sum_{j=1}^{n} V_{j,k_{(y,d)}} \times \left[G_{i,j}\cos\left(\delta_{i,j,k_{(y,d)}}\right) + B_{i,j}sin\left(\delta_{i,j,k_{(y,d)}}\right)\right] \quad (15)$$

$$Q_{i,k_{(y,d)}} = V_{i,k_{(y,d)}} \sum_{j=1}^{n} V_{j,k_{(y,d)}} \left[G_{i,j}\sin\left(\delta_{i,j,k_{(y,d)}}\right) - B_{i,j}cos\left(\delta_{i,j,k_{(y,d)}}\right)\right]$$
$$i = 1, \ldots, n, \quad k = 1, \ldots, nt, \quad y = 1, \ldots, ny, \quad d = 1, \ldots, nd_y \quad (16)$$

where $\delta_{i,j,k_{(y,d)}} = \delta_{i,k_{(y,d)}} - \delta_{j,k_{(y,d)}}$ and, with reference to the time interval k of the day d, year y, $P_{i,k_{(y,d)}}$ ($Q_{i,k_{(y,d)}}$) is the net active (reactive) power injected at the bus i, $V_{j,k_{(y,d)}}$ ($\delta_{\mathrm{i,k}_{(y,d)}}$) is the magnitude (argument) of the bus voltage, $G_{i,j}(B_{i,j})$ is the (i,j)-term of the system's conductance (susceptance) matrix and n is the number of μG buses. The bus #1, that is the bus where the μG is connected to the upstream network is assumed as slack bus:

$$V_{1,k_{(y,d)}} = V_{spec} \quad (17)$$
$$\delta_{1,k_{(y,d)}} = 0 \qquad k=1, \ldots, nt, \quad y=1, \ldots, ny, \ d=1, \ldots, nd_y \quad (18)$$

In (15) and (16), active and reactive powers are given by the sum of the powers of the loads, the power of the EESSs (in busses where they are connected) and the power of the DG units (in busses where they are connected). As an example, if at the generic bus i load, EESS and DG are connected, the net active and reactive power at that bus is subject to the following equality constraints:

$$P_{i,k_{(y,d)}} = P_{ld,i,k_{(y,d)}} + P_{b,i,k_{(y,d)}} + P_{dg,i,k_{(y,d)}} \tag{19}$$

$$Q_{i,k_{(y,d)}} = Q_{ld,i,k_{(y,d)}} + Q_{b,i,k_{(y,d)}} + Q_{dg,i,k_{(y,d)}}$$
$$k = 1, \ldots, nt, \quad y = 1, \ldots, ny, \; d = 1, \ldots, nd_y \tag{20}$$

where $P_{ld,i,k_{(y,d)}}$ and $Q_{ld,i,k_{(y,d)}}$ are the active and reactive power, respectively, requested by the load, $P_{b,i,k_{(y,d)}}$ is the active power of the EESS (at this step it is a specified value provided by sub-section A), $P_{dg,i,k_{(y,d)}}$ is the active power of the DG unit (assumed as positive,) at this step it is a specified value provided by forecasting, $Q_{b,i,k_{(y,d)}}$ and $Q_{dg,i,k_{(y,d)}}$ are the reactive power of the EESS and DG, respectively, which are optimization variables.

Inequality constraints apply on the active and reactive power flowing through the transformers and converters included in the μG. In the case of the transformers which are used to supply feeders, their apparent powers cannot exceed the rated power:

$$\left[\left(P_{v,k_{(y,d)}}\right)^2 + \left(Q_{v,k_{(y,d)}}\right)^2\right]^{1/2} \leq S^{rtd}_{tr,v}$$
$$v \in \Omega_{tr}, k = 1, \ldots, nt, y = 1, \ldots, ny, d = 1, \ldots, nd_y \tag{21}$$

where $P_{v,k_{(y,d)}}(Q_{v,k_{(y,d)}})$ is the active (reactive) power flowing through the vth transformer, $S^{rtd}_{tr,v}$ is its rated power and Ω_{tr} is the set of transformers. In the case of converters, which are used to connect EESSs and DG units, the apparent power cannot exceed the converter rated power:

$$\left[\left(P_{b,i,k_{(y,d)}}\right)^2 + \left(Q_{b,i,k_{(y,d)}}\right)^2\right]^{1/2} \leq S^{rtd}_{DESS,i} \quad i \in \Omega_{DESS} \tag{22}$$

$$\left[\left(P_{dgi,k_{(y,d)}}\right)^2 + \left(Q_{dg,i,k_{(y,d)}}\right)^2\right]^{1/2} \leq S^{rtd}_{DG,i} \quad i \in \Omega_{DG}$$
$$k = 1, \ldots, nt, \quad y = 1, \ldots, ny, \; d = 1, \ldots, nd_y \tag{23}$$

where $S^{rtd}_{DESS,i}$ is the rated power of the converter of the EESS, $S^{rtd}_{DG,i}$ is the rated power of the converter of the DG unit, Ω_{DESS} is the set of buses where EESSs are connected and Ω_{DG} is the set of buses where DG units are connected.

Note that, the provision of the reactive power affects the battery capacity in terms of the additional active power losses implied by the conversion system. Losses in the conversion device are supplied by the storage itself, thus implying a reduction of the SOC [45]. In order to evaluate these additional losses different approximated methods can be used, which are based on polynomial function of the apparent power flowing through the converter [14], [46]. These approaches imply further approximations due to the need of accurate estimation of the parameters included in the polynomial function, whose values depend on battery technology and size as well as on its operative condition. In the proposed approach the storage device has been modeled in terms of the efficiency affecting the active power provision and SOC while its interface to the grid is characterized by active and reactive power capability limits.

In order to guarantee a correct operation of the μG, an inequality constraint is imposed on the voltage magnitude of all the busses of the μG, which must fall within admissible range:

$$V_{min} \leq V_{i,k_{(y,d)}} \leq V_{max}$$
$$k=1, \ldots, nt, \quad y=1, \ldots, ny, \; d=1, \ldots, nd_y \tag{24}$$

where $V_{min}(V_{max})$ is the minimum (maximum) value that the bus voltage magnitude can assume at the generic bus i. Moreover, line currents cannot exceed a maximum value imposed by the line ampacity:

$$I_{l,k_{(y,d)}} \leq I_{l,max}$$
$$l \in \Omega_l, \quad k = 1, \ldots, nt, \; y = 1, \ldots, ny, \; d = 1, \ldots, nd_y \tag{25}$$

where Ω_l is the set of the line of the μG, $I_{l,k_{(y,d)}}$ is the current flowing through the lth line and $I_{l,max}$ is its ampacity. Line current can be derived from the bus voltages at the starting and arrival ends of the line, which are optimization variables.

A further constraint can be imposed in order to limit the power imported by the μG within an admissible maximum value (P_{max}):

$$P_{1,k_{(y,d)}} \leq P_{\max}$$
$$k = 1, \ldots, nt, \quad y = 1, \ldots, ny, \; d = 1, \ldots, nd_y \tag{26}$$

In order to solve the proposed OPF, the sequential quadratic programming (SQP) method is used in the numerical applications. In particular, the optimization toolbox of Matlab [47] has been adopted and, more specifically, the function '*fmincon*'. This function finds minimum of constrained nonlinear multivariable function by using an SQP method which iteratively solves a quadratic programming subproblem and performing a line search using a merit function similar to that proposed by [48]. Use of the initial point value within an operational region, which is inherently very limited, allows approaching the physical optimum.

IV. DECISION THEORY CRITERIA

When uncertain inputs affect the decision problem, several approaches can be applied to select the best alternatives [37], [49]. In this paper, some criteria based on the decision theory are proposed to select the alternatives which show the best performances over the considered futures; these criteria are shown in the following sub-sections.

As already mentioned in the previous section, a set of design alternatives is available ($A_p, p = 1, \ldots, na$) as well as a set of futures ($F_q, q = 1, \ldots, nf$) that can occur. The DM also assigns a value of probability of occurrence to each future ($\omega_q, q = 1, \ldots, nf$). The sum of the nf values is unitary.

For each design alternative A_p, the total cost, $C_T\left(A_p, F_q\right)$, related to the inclusion of EESSs in the μG when future F_q occurs has been evaluated by (1), applying the procedure shown in Section III. These values are often provided in a matrix, referred to as decision matrix.

A. CRITERION OF THE EXPECTED COST MINIMIZATION

This first criterion is based on the minimization of the expected total costs. For each alternative, A_p, the expected total cost [37] associated with all the nf futures is evaluated as:

$$EC_T\left(A_p\right) = \sum_{q=1}^{nf} \omega_q C_T\left(A_p, F_q\right) \quad p = 1, \ldots, na \tag{27}$$

The best alternative $A_{opt,ec}$ among all the na alternatives is the one associated with the lowest value of the expected total costs (27). The criterion of the expected cost minimization suggests design alternatives which are the best on the average of the futures so that if the future which really occurred does not happen close to the average, high regrets can derive.

B. CRITERION OF MIN-MAX WEIGHTED REGRET

The second criterion is based on the minimization of the maximum weighted regrets [38]. The regret can be defined as follows: once known the future occurred, the DM can evaluate the regret felt when the optimal decision for the really occurred future was not made.

For each future, the minimum total cost can be easily found as:

$$C_T^{opt}\left(F_q\right) = \min_p C_T\left(A_p, F_q\right) \quad q = 1, \ldots, nf \tag{28}$$

After that, the regret $R\left(A_p, F_q\right)$ felt for having chosen the design alternative A_p when the future F_q occurred is:

$$R\left(A_p, F_q\right) = C_T\left(A_p, F_q\right) - C_T^{opt}\left(F_q\right) \qquad p = 1, \ldots, na, \quad q = 1, \ldots, nf \tag{29}$$

and the weighted regret $R_w\left(A_p, F_q\right)$ is:

$$R_w(A_p, F_q) = \omega_q R(A_p, F_q) \quad p = 1, \ldots, na, \quad q = 1, \ldots, nf \tag{30}$$

For each design alternative, the maximum weighted regret can be identified as:

$$R_w^{max}\left(A_p\right) = \max_q R_w\left(A_p, F_q\right) \quad p = 1, \ldots, na \tag{31}$$

Then, the best alternative $A_{opt,r}$ among all the na alternatives is the one associated with the minimum among the maximum weighted regrets (31).

As a general comment, it is worth noting that when the DM minimizes the maximum weighted regret, design alternatives which have not good performances in any considered future are excluded. Considering regrets instead of total expected costs, the decisions may be less risky and design alternatives with higher value of the costs can be selected.

C. CRITERION BASED ON STABILITY AREAS

The solutions provided by the decision criteria described in subsections A and B are clearly affected by the assignment of the probabilities of occurrence of each future; in fact, both the expected costs and the weighted regrets depend on the values of ω_q, $q = 1, \ldots, nf$.

To overcome difficulties related to probability assignment, the concept of the stability areas can be introduced. First proposed in [38] and [50], the stability areas aimed at evaluating the range of future probabilities in which the solutions are stable. If the probabilities of occurrence of each future are considered as variable parameters, a large number of set of future probabilities can be considered and for each set the decision criteria can be applied. More specifically, for each set of future probabilities ($s = 1, \ldots, ns$), the criterion of the expected cost minimization and the criterion of min-max weighted regret will be separately applied and will provide the design solution $A^s_{opt,ec}$ and $A^s_{opt,r}$ to be chosen associated to the set s.

The DM can select the best design alternative as the design alternative which is more frequently provided as the optimal solution. This is referred to as criterion of the maximum stability areas. Moreover, the design solutions suggested by the applied decision criteria can coincide or differ. A further decision criterion can, then, be established: for each set of future probabilities ($s = 1, \ldots, ns$), only if the solutions provided by the criterion of the expected cost minimization and the criterion of min-max weighted regret coincide, the solution is considered, otherwise the solutions will be discarded. When all the sets ns are considered, the DM could select the design alternative with the highest frequency.

If the number of futures nf is equal to three, the stability areas can have triangular graphical representations related to different criteria. When the number of futures nf is greater than three, it will be better to provide a graphical representation based on histograms, as it will be shown in the next Section of Numerical Applications.

V. NUMERICAL APPLICATION

The proposed method has been applied to an MV μG considering as uncertainties load and DG power levels. The μG considered for the numerical application is the three-phase, balanced, distribution network of Fig. 2. This network refers to the MV Cigrè benchmark system detailed in [51] whose nominal voltage is 12.47 kV. It includes 15 busses and is connected to a 115 kV grid by means of two transformers of 25 MVA (whose primary and secondary sides are connected to bus #1 and bus #2) and 20 MVA (bus #1 and bus #13), respectively. These transformers supply two feeders to whom residential, industrial and commercial loads are connected (feeder #1 and feeder #2).

The load data, which include locations, rated powers and power factors, are detailed in Tab. 1. Two typical days are considered for each year. Examples of daily profiles of the commercial/industrial and residential loads are shown in Fig. 3

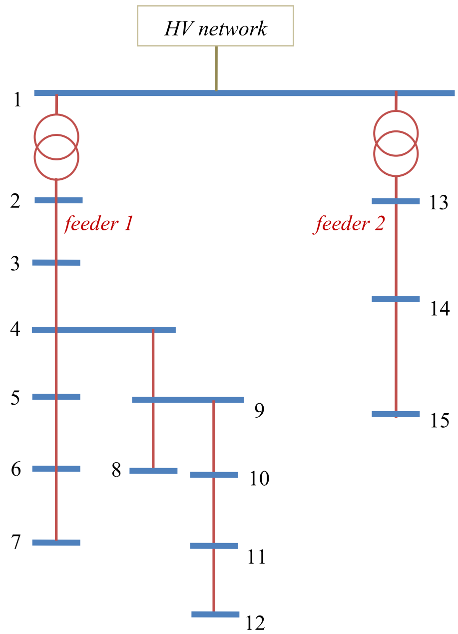

FIGURE 2. MV Cigrè benchmark system.

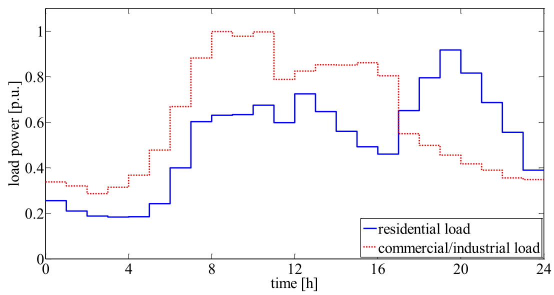

FIGURE 3. Daily profile of the comm./industrial and residential loads [51].

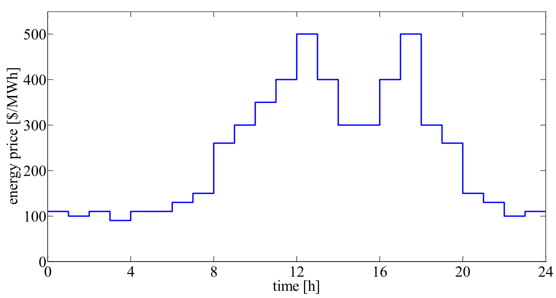

FIGURE 4. Energy price [52].

TABLE 1. Load input data.

Bus #	Rated power (MVA)	Load type	cos φ
2	13.8	Residential	0.93
	9.16	Comm./industrial	0.87
3	0.35	Residential	0.95
	0.80	Comm./industrial	0.85
4	0.25	Residential	0.90
	0.24	Comm./industrial	0.80
5	0.40	Residential	0.90
6	0.20	Residential	0.95
	0.30	Comm./industrial	0.85
7	0.15	Residential	0.95
8	0.10	Residential	0.95
	0.30	Comm./industrial	0.95
9	0.25	Residential	0.90
	0.20	Comm./industrial	0.90
10	0.35	Residential	0.95
11	0.50	Residential	0.90
12	0.10	Residential	0.95
	0.45	Comm./industrial	0.85
13	3.20	Residential	0.90
	3.78	Comm./industrial	0.87
14	0.68	Comm./industrial	0.85
15	0.27	Comm./industrial	0.90

TABLE 2. Definition of the futures.

Future #	Load level	DG
1	70%	-
2		5 MW @ bus 9
3		5 MW @ bus 9 and 2 MW @ bus 15
4	80%	-
5		5 MW @ bus 9
6		5 MW @ bus 9 and 2 MW @ bus 15
7	90%	-
8		5 MW @ bus 9
9		5 MW @ bus 9 and 2 MW @ bus 15

[51]. Regarding the price of energy, the energy pricing tariff, whose hourly values are available in [52] and are reported in Fig. 4, has been used. By observing the price profile in Fig. 4, it appears convenient that the EESSs is discharged in the hours from 8:00 to 20:00 (i.e., when prices are highest) and is charged in the rest of the day.

We considered 9 futures which refer to:

- the first year load demand that can be equal to 70%, 80% or 90% of the rated powers reported in Tab. I;
- no DG, one DG (5 MW @ bus #9), two DG (5 MW @ bus #9 and 2 MW @ bus #15). The DG units are photovoltaic (PV) systems.

The futures are defined in Table 2. For each future, an annual growth of the load (2.5%) and energy prices (1%) have been considered. The planning time horizon has been assumed of 20 years.

The design alternatives have been indentified in terms of number of EESSs to be allocated, their sizes and allocation buses. Regarding the number, a maximum of three EESSs can

TABLE 3. EESS data.

Parameter	Value
Charging efficiency	92%
Discharging efficiency	95%
Maximum Depth of Discharge	80%
Cycle life	4000
Installation cost	600 $/kWh

be allocated. Their sizes can be chosen among the set Ω_{size}, whose values are:

$$\Omega_{size} = \{0, 0.25, 0.5, 2.5, 5\}\, MW \tag{32}$$

with a nominal discharging time of five hours. The EESSs considered in this application are equipped with Li-ion batteries, whose performance features depend on different parameters related to chemistry properties, cell design and operating conditions [53]. The data of the EESS used in this application have been derived from [53] and adapted as reported in Tab. 3. One battery replacement was considered over the planning period, for which, a cost of 50% of that required in the first installation was assumed [54].

In order to reduce the number of candidate busses, two tools are used, which are based on the inherent structure theory of networks and the loading constraints criterion [18], [55]–[58]. The former is used to select those busses where the effect of the net injection of power from energy resources (in this case EESSs) allows obtaining the largest effects than the others; the latter refers to those busses where the net injection of power from resources implies the reduction of the power flowing through the lines during the most critical events. In both cases, the number of selected busses are defined according to specified threshold values [55]–[58]. The resulting set of candidate busses, $\Omega_{candidate}$, is:

$$\Omega_{candidate} = \{2, 3, 4, 8, 11, 12, 14, 15\} \tag{33}$$

In particular, the busses included in (33) correspond to the threshold values of 35% for the inherent structure theory of networks [55]–[58] and 80% for the loading constraints criterion [58]. Each design alternative corresponds to three EESSs whose rated power is one of those included in the set Ω_{size}, allocated in three of the busses included in the set $\Omega_{candidate}$. The number of all of the alternatives is then 6125 which have to be analyzed for each of the nine futures. In what follows, the design alternatives are referred to as A_p with $p = 1, \ldots, 6125$. The large number of design alternatives and futures to be analyzed must not be discouraging, since the proposed minimum cost strategy is efficiently solved for each alternative in few seconds.

The results of two case studies are reported:

case 1) futures #4, #5 and #6 are analyzed; they correspond to the case of 80% load power at the first year and three scenarios of DG; in this very simple case, the stability area criterion has a very simple graphical representation and, then, the proposed approach can be more easily illustrated.

case 2) all nine futures are analyzed.

In both cases, the criteria presented in Section IV are applied and discussed in the following sub-Sections.

TABLE 4. Design alternatives resulting from the minimum total cost and min-max regrets (case 1).

Alternative	EESS # 1		EESS # 2		EESS # 3	
	bus #	size (MW)	bus #	size (MW)	bus #	size (MW)
A_{1474}	2	5	8	5	14	2.5

A. CASE 1

Considering the performances of the design alternatives in each future, a decision matrix of 6125x3 elements was built, that is the total cost corresponding to the 6125 design alternatives evaluated at the futures 4, 5 and 6 of Tab. 2. It should be considered, however, that in the applications of the minimum cost strategy, the set of constraints (15)-(26) have to be met. In the case the OPF of a design alternative does not converge, due to the imposed constraints, in at least one future, the alternative has to be discarded. After this verification, in this application the decision matrix was reduced to 5762x3 elements, since 363 did not satisfy the constraints in at least one future. This matrix is not reported here for the sake of brevity.

When each future is considered to have the same probability (i.e., 1/3), the criterion of the minimum expected costs provides the design alternative A_{1474} as the optimal solution with an expected minimum cost of 9.5 M$. Still referring to the futures considered with the same probability, the criterion of the min-max weighted regrets still provides the design alternative A_{1474} as the optimal solution. This solution is detailed in Tab. 4. The solution refers to the allocation of two EESSs in the first feeder (busses #2 and #8) each of rated power of 5 MW, and one EESS allocated at the second feeder (bus #14) with a rated power of 2.5 MW.

Still referring to the three futures #4, #5 and #6, the stability areas can be graphically shown as in Fig. 5. In particular, Fig. 5 a) and b) show the stability areas obtained by applying the criteria of expected cost minimization and of min-max weighted regrets, respectively. In Fig. 5 c), only the couples of probabilities for which both the decision criteria provide the same optimal solution are shown.

By analyzing Fig. 5, a significant amount of information on the planning problem can be derived to aid the DM select the best design alternative. In particular, in Figs. 5 a) and 5 b), four design alternatives are always selected by applying the criteria of the minimum expected costs and the min max weighted regrets, respectively while varying the future probabilities. In Fig. 5 c) the area with the alternative that occurs with the largest frequency is the A_{1474} (about 69%). It clearly appears that other solutions were characterized by

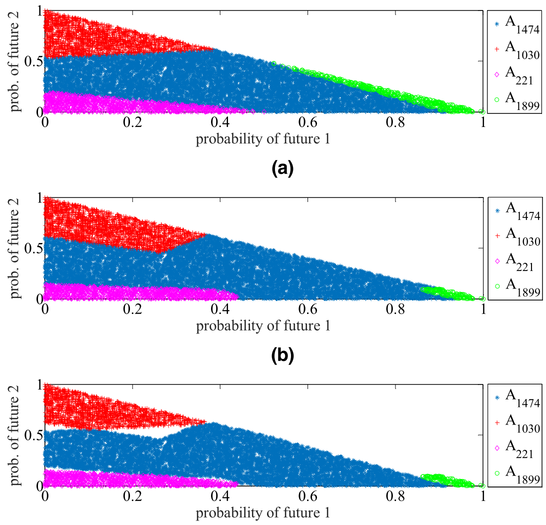

FIGURE 5. Stability areas: Criterion of minimum expected costs (a), criterion of min max weighted regrets (b), both minimum expected costs and min max weighted regrets criteria (c).

TABLE 5. Design alternatives provided by the Stability areas (case 1).

Alternative	EESS # 1		EESS # 2		EESS # 3	
	bus #	size (MW)	bus #	size (MW)	bus #	size (MW)
A_{1474}	2	5	8	5	14	2.5
A_{1030}	2	2.5	4	5	14	5
A_{221}	2	5	3	2.5	8	5
A_{1899}	2	5	11	5	15	2.5

smaller stability areas: 17% of the trials gave the preferred solution as A_{1030}, 10% of the trials gave the preferred solution as A_{221} and 4% of the trials gave the preferred solution as A_{1899}. Details on these solutions, in terms of siting and size of the EESSs are described in Tab. 5.

The results shown in Tab. 5 are coherent with that resulting from the applications of the two minimum cost and min-max regrets criteria when the same probability is considered for the three futures. In fact, the solutions reported in Tab. 5 show that it is always convenient to install an EESS at the bus #2. This is probably due to the features of the load demand that do not change in the three futures. Clearly, based on the probabilities the DM would assign to each future (which refer to different penetration levels of DG units), a different allocation solution can be derived by the analysis of Fig. 5.

B. CASE 2

In this case all of the futures in Tab. 2 are analyzed. By considering the performances of the design alternatives in each future, a decision matrix of 6125x9 elements has been built. In this case, also, design alternatives which do not satisfy all the constraints of the proposed minimum cost strategy in at least one future have been discarded. After this verification, the decision matrix was reduced to 5469x9 elements.

TABLE 6. Details of relevant design alternatives in case 2.

Alternative	EESS # 1		EESS # 2		EESS # 3	
	bus #	size (MW)	bus #	size (MW)	bus #	size (MW)
A_{1697}	2	5	11	5	12	0.25
A_{1472}	2	5	8	5	14	0.25

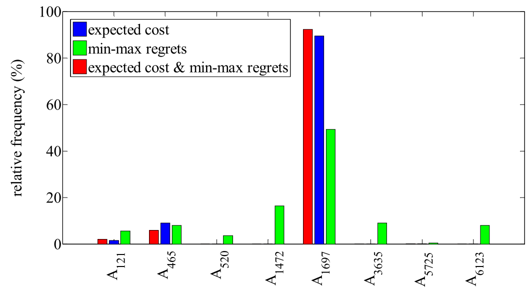

FIGURE 6. Stability areas by applying criterion of minimum expected costs, criterion of min max weighted regrets, both minimum expected costs and min max weighted regrets criteria.

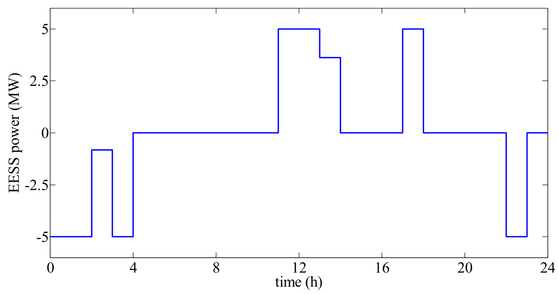

FIGURE 7. Daily profile of the active power of the EESS located at the bus #2.

When the futures are considered with the same probability (i.e., 1/9), the criterion of the minimum expected costs provides the design alternative A_{1697} as the optimal solution with an expected minimum cost of 9.8 M$, while the criterion of the min-max weighted regrets provides the design alternative A_{1472} as the optimal solution. Both these solutions, are detailed in Tab. 6.

In Tab. 6 it can be observed that the allocation of an EESS in the bus #2 provides beneficial effects with reference to both minimum expected cost and min-max regrets criteria. Moreover, the installation of EESSs resulting from the minimum expected cost criterion is that corresponding to the installation of EESSs only in the first feeder. Compared to the min-max regrets criterion, the minimum expected cost criterion implies a solution with a slightly lower total EESS rated powers.

In this case study, the histograms obtained by applying the criteria of expected cost minimization and of min-max weighted regrets are reported in Fig. 6. Moreover, the cases of probabilities for which both the decision criteria provide

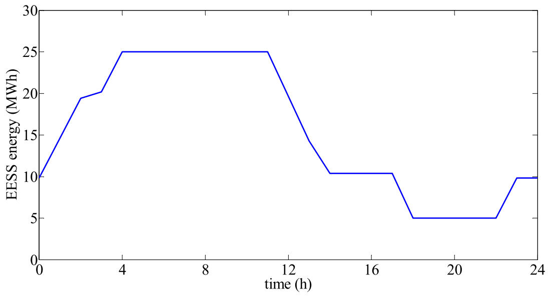

FIGURE 8. Daily profile of the energy stored in the EESS located at the bus #2.

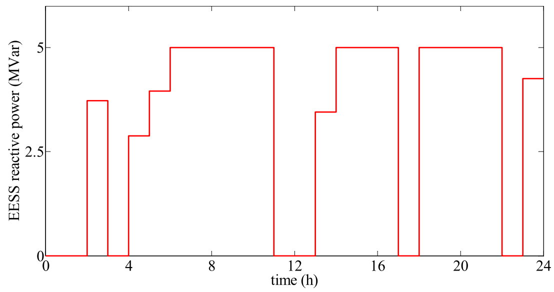

FIGURE 9. Daily profile of the reactive power of the EESS located at the bus #2.

TABLE 7. Details of relevant design alternatives in case 2.

Alternative	EESS # 1		EESS # 2		EESS # 3	
	bus #	size (MW)	bus #	size (MW)	bus #	size (MW)
A_{1697}	2	5	11	5	12	0.25
A_{1472}	2	5	8	5	14	0.25
A_{3635}	3	5	12	0.25	14	5
A_{6123}	12	5	14	5	15	0.5
A_{465}	2	0.25	3	5	14	5
A_{121}	2	5	3	5	-	-
A_{520}	2	5	3	2.5	14	2.5
A_{5725}	11	0.5	12	5	14	5

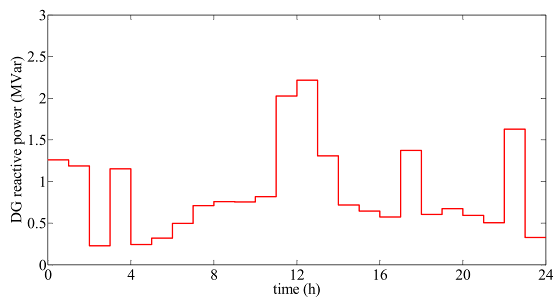

FIGURE 10. Daily profile of the reactive power of the DG located at the bus #9.

the same optimal solution are also reported. As it can be seen, the three criteria provide the alternative A_{1697} as that corresponding to the maximum relative frequency. Particularly, the relative frequency is 89.5% in case of the minimum expected cost criterion, 49.2% in case of min-max weighted regrets and 93.6% in case of both criteria adopted. In Fig. 6 it can also be observed that several design alternatives have been identified as optimal solutions while probabilities vary, even if with lower values of relative frequencies. In particular, it is interesting to note that, most of these alternatives have been identified through the application of the min-max weighted regrets. The alternatives in Fig. 6 are detailed in Tab. 7 where, compared to the case 1, a wider range of solutions is shown. This was expected based on the greater number of futures considered.

In Tab. 7, it can be observed that some solutions do not include the connection of EESSs at bus #2 (A_{3635}, A_{6123} and A_{5725}). In these cases, compared to the other solutions, a reduced overall energy capacity is allocated at the first feeder. Moreover, in one solution (A_{121}) only two EESSs are allocated.

With reference to the solution A_{1697} in Figs. 7-12 some details of the proposed minimum cost strategy are reported, with reference to the last year of the planning period of the future #6. More specifically, the active power daily profile of the EESS located at bus #2 is reported in Fig. 7; its stored energy is shown in Fig. 8; the reactive power of the storage located at the bus #2 is reported in Fig. 9; in Fig. 10 the reactive power of the DG located at the bus #9 is shown; examples of bus voltages and line currents are reported in Figs. 11 and 12, respectively.

Coherently with the objective of cost reduction, Fig. 7 shows that the EESS is discharged in the high price hours and is charged during the low price hours (see Fig. 4). The constraints in terms of rated power and energy capacity are satisfied, as clearly shown in Fig. 8. Moreover, from Figs. 7 and 8, it can be observed that the EESS is fully exploited in terms of rated power (5 MW) and energy capacity (25 MWh); the maximum depth of discharge (80%) and the limit of one charging/discharging cycle per day is also satisfied. Regarding the reactive power, Fig. 9 clearly shows that the EESS always is used for providing the maximum reactive power compatible with the provided active power. Indeed, when the EESS provides active power (see Fig. 7), the reactive power is reduced or is null due to the limitation on the apparent power which cannot exceed the rated power of the interfacing converter. Also the DG units, as shown in Fig. 10, provide high share of reactive power.

Figs. 11 and 12 show that the proposed procedure allows satisfying the constraints on the voltages and currents. More in details, in Fig. 11 the bus voltage at the hours with highest voltage values (hour 14) and lowest voltage values (hour 23) are reported.

In both profiles of Fig. 11, the voltage is always within the admissible range (0.9-1.1 p.u.). The line currents in all the

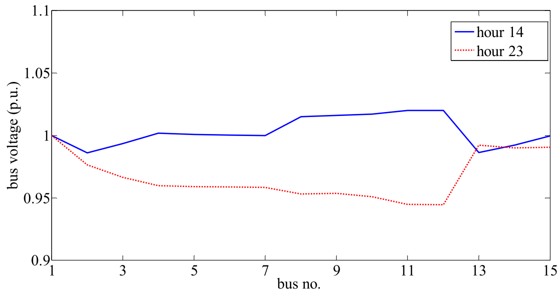

FIGURE 11. Bus voltage at the network buses at hours 14 and 23.

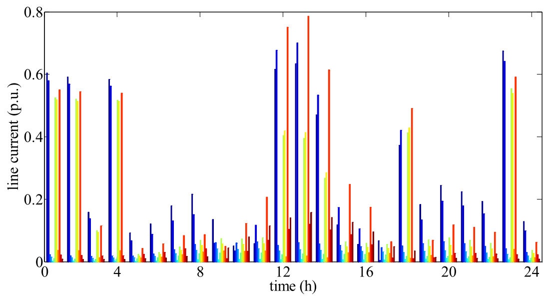

FIGURE 12. Line currents during the whole day.

hours of the day are shown in Fig. 12. The values are reported in p.u. with respect to the lines' ampacities. As clearly shown in the figure, all the currents always are lower than the maximum admissible value.

VI. CONCLUSIONS

In this paper a planning method has been proposed for the optimal sizing and siting of electrical energy storage systems in a microgrid in the presence of renewable energy sources. Uncertainties of loads and generation are handled by means of decision theory criteria. The optimal planning allows reducing the costs for energy provision and supplying technical support to the grid. The proposed method includes a novel minimum cost strategy, which is tailored for the case of hourly varying pricing scheme. This method allowed optimizing active and reactive power of storage devices and reactive power of renewable generation in an effective way, while preserving the computational effectiveness which is crucial when dealing with planning involving uncertainties and storage devices due to the multi-temporal nature of the problem. The results of numerical applications, derived with respect to a Cigré test network, clearly showed the feasibility and effectiveness of the procedure. This demonstrated that the proposed approach is useful to a microgrid operator who wants to exploit the advantages of the storage in terms of demand response applications. Based on the proposed approach, current research activity has been focusing on the development of more detailed models to characterize battery degradation. The aim is to study the effect of some parameters, such as ambient temperature, in the evaluation of the costs related to the planning of battery energy storage systems. Furthermore, models of the energy storage systems will be explored to accurately include the reactive power capability while preserving computation efficiency of the planning method.

REFERENCES

[1] G. Strbac *et al.*, "Opportunities for energy storage: Assessing whole-system economic benefits of energy storage in future electricity systems," *IEEE Power Energy Mag.*, vol. 15, no. 5, pp. 32–41, Sep./Oct. 2017, doi: 10.1109/MPE.2017.2708858.

[2] X. Yan, C. Gu, F. Li, and Y. Xiang, "Network pricing for customer-operated energy storage in distribution networks," *Appl. Energy*, vol. 212, pp. 283–292, Feb. 2018, doi: 10.1016/j.apenergy.2017.12.060.

[3] Z. Chen, L. Wu, and Y. Fu, "Real-time price-based demand response management for residential appliances via stochastic optimization and robust optimization," *IEEE Trans. Smart Grid*, vol. 3, no. 4, pp. 1822–1831, Dec. 2012, doi: 10.1109/TSG.2012.2212729.

[4] G. Carpinelli, F. Mottola, D. Proto, and A. Russo, "A multi-objective approach for microgrid scheduling," *IEEE Trans. Smart Grid*, vol. 8, no. 5, pp. 2109–2118, Sep. 2017, doi: 10.1109/TSG.2016.2516256.

[5] C. Chen, S. Duan, T. Cai, B. Liu, and G. Hu, "Optimal allocation and economic analysis of energy storage system in microgrids," *IEEE Trans. Power Electron.*, vol. 26, no. 10, pp. 2762–2773, Oct. 2011, doi: 10.1109/TPEL.2011.2116808.

[6] Z. Qiao and J. Yang, "Comparison of centralised and distributed battery energy storage systems in LV distribution networks on operational optimisation and financial benefits," *J. Eng.*, vol. 2017, no. 13, pp. 1671–1675, 2017, doi: 10.1049/joe.2017.0616.

[7] G. Carpinelli, F. Mottola, D. Proto, and P. Varilone, "Minimizing unbalances in low-voltage microgrids: Optimal scheduling of distributed resources," *Appl. Energy*, vol. 191, pp. 170–182, Apr. 2017, doi: 10.1016/j.apenergy.2017.01.057.

[8] R. Moreira, G. Strbac, P. Papadopoulos, and A. Laguna, "Business case in support for reactive power services from distributed energy storage," in *Proc. 24th Int. Conf. Exhib. Electr. Distrib.*, Glasgow, Scotland, Jun. 2017, pp. 1–5.

[9] A. Ahmadian, M. Sedghi, and M. Ałiakbar-Golkar, "Fuzzy load modeling of plug-in electric vehicles for optimal storage and DG planning in active distribution network," *IEEE Trans. Veh. Technol.*, vol. 66, no. 5, pp. 3622–3631, May 2017, doi: 10.1109/TVT.2016.2609038.

[10] M. Daghi, M. Sedghi, A. Ahmadian, and M. Aliakbar-Golkar, "Factor analysis based optimal storage planning in active distribution network considering different battery technologies," *Appl. Energy*, vol. 183, 2016, pp. 456–469, Dec. 2016, doi: 10.1016/j.apenergy.2016.08.190.

[11] F. Mottola, D. Proto, A. Russo, and P. Varilone, "Planning of energy storage systems in unbalanced microgrids," in *Proc. IEEE PES Innov. Smart Grid Technol. Conf. Eur. (ISGT-Europe)*, Turin, Italy, Sep. 2017, pp. 1–6.

[12] Y. Zheng, Z. Dong, F. J. Luo, K. Meng, J. Qiu, and K. P. Wong, "Optimal allocation of energy storage system for risk mitigation of DISCOs with high renewable penetrations," *IEEE Trans. Power Syst.*, vol. 29, no. 1, pp. 212–220, Jan. 2014, doi: 10.1109/TPWRS.2013.2278850.

[13] J. Qiu, J. Zhao, Y. Zheng, Z. Dong, and Z. Y. Dong, "Optimal allocation of BESS and MT in a microgrid," *IET Gener., Transmiss. Distrib.*, vol. 12, no. 9, pp. 1988–1997, May 2018, doi: 10.1049/iet-gtd.2017.0717.

[14] M. Nick, R. Cherkaoui, and M. Paolone, "Optimal siting and sizing of distributed energy storage systems via alternating direction method of multipliers," *Int. J. Elect. Power Energy Syst.*, vol. 72, pp. 33–39, Nov. 2015, doi: 10.1016/j.ijepes.2015.02.008.

[15] M. Motalleb, E. Reihani, and R. Ghorbani, "Optimal placement and sizing of the storage supporting transmission and distribution networks," *Renew. Energy*, vol. 94, pp. 651–659, Aug. 2016, doi: 10.1016/j.renene.2016.03.101.

[16] E. Grover-Silva, R. Girard, and G. Kariniotakis, "Optimal sizing and placement of distribution grid connected battery systems through an SOCP optimal power flow algorithm," *Appl. Energy*, vol. 219, pp. 385–393, Jun. 2018, doi: 10.1016/j.apenergy.2017.09.008.

[17] C. P. Delgado-Antillón and J. A. Domínguez-Navarro, "Probabilistic siting and sizing of energy storage systems in distribution power systems based on the islanding feature," *Electr. Power Syst. Res.*, vol. 155, pp. 225–235, Feb. 2018, doi: 10.1016/j.epsr.2017.10.013.

[18] G. Carpinelli, F. Mottola, D. Proto, A. Russo, and P. Varilone, "A hybrid method for optimal siting and sizing of battery energy storage systems in unbalanced low voltage microgrids," *Appl. Sci.*, vol. 8, no. 3, p. 455, 2018, doi: 10.3390/app8030455.
[19] G. Carpinelli, G. Celli, S. Mocci, F. Mottola, F. Pilo, and D. Proto, "Optimal integration of distributed energy storage devices in smart grids," *IEEE Trans. Smart Grid*, vol. 4, no. 2, pp. 985–995, Jun. 2013, doi: 10.1109/TSG.2012.2231100.
[20] G. Carpinelli, F. Mottola, D. Proto, and A. Russo, "Optimal allocation of dispersed generators, capacitors and distributed energy storage systems in distribution networks," in *Proc. Modern Electr. Power Syst.*, Wroclaw, Poland, Sep. 2010, pp. 1–6.
[21] W. Li, C. Lu, X. Pan, and J. Song, "Optimal placement and capacity allocation of distributed energy storage devices in distribution networks," in *Proc. 13th IEEE Conf. Autom. Sci. Eng.*, Xi'an, China, Aug. 2017, pp. 1403–1407.
[22] M. Nick, R. Cherkaoui, and M. Paolone, "Optimal planning of distributed energy storage systems in active distribution networks embedding grid reconfiguration," *IEEE Trans. Power Syst.*, vol. 33, no. 2, pp. 1577–1590, Mar. 2018, doi: 10.1109/TPWRS.2017.2734942.
[23] V. Kalkhambkar, R. Kumar, and R. Bhakar, "Joint optimal allocation methodology for renewable distributed generation and energy storage for economic benefits," *IET Renew. Power Gener.*, vol. 10, no. 9, pp. 1422–1429, Oct. 2016, doi: 10.1049/iet-rpg.2016.0014.
[24] C. Chen and S. Duan, "Optimal allocation of distributed generation and energy storage system in microgrids," *IET Renew. Power Gener.*, vol. 8, no. 6, pp. 581–589, Aug. 2014, doi: 10.1049/iet-rpg.2013.0193.
[25] G. Carpinelli, F. Mottola, C. Noce, A. Russo, and P. Varilone, "A new hybrid approach using the simultaneous perturbation stochastic approximation method for the optimal allocation of electrical energy storage systems," *Energies*, vol. 11, no. 6, p. 1505, 2018, doi: 10.3390/en11061505.
[26] Q. Sun, B. Huang, D. Li, D. Ma, and Y. Zhang, "Optimal placement of energy storage devices in microgrids via structure preserving energy function," *IEEE Trans. Ind. Informat.*, vol. 12, no. 3, pp. 1166–1179, Jun. 2016, doi: 10.1109/TII.2016.2557816.
[27] M. Sedghi, A. Ahmadian, and M. Aliakbar-Golkar, "Optimal storage planning in active distribution network considering uncertainty of wind power distributed generation," *IEEE Trans. Power Syst.*, vol. 31, no. 1, pp. 304–316, Jan. 2016, doi: 10.1109/TPWRS.2015.2404533.
[28] A. Ahmadian, M. Sedghi, M. Aliakbar-Golkar, A. Elkamel, and M. Fowler, "Optimal probabilistic based storage planning in tap-changer equipped distribution network including PEVs, capacitor banks and WDGs: A case study for Iran," *Energy*, vol. 112, pp. 984–997, Oct. 2016, doi: doi.org/10.1016/j.energy.2016.06.132.
[29] S. Wang, K. Wang, F. Teng, G. Strbac, and L. Wu, "Optimal allocation of ESSs for mitigating fluctuation in active distribution network," *Energy Procedia*, vol. 142, pp. 3572–3577, Dec. 2017, doi: 10.1016/j.egypro.2017.12.247.
[30] P. Xiong and C. Singh, "Optimal planning of storage in power systems integrated with wind power generation," *IEEE Trans. Sustain. Energy*, vol. 7, no. 1, pp. 232–240, Jan. 2016, doi: 10.1109/TSTE.2015.2482939.
[31] R. Li, W. Wang, Z. Chen, and X. Wu, "Optimal planning of energy storage system in active distribution system based on fuzzy multi-objective bi-level optimization," *J. Mod. Power Syst. Clean Energy*, vol. 6, no. 2, pp. 342–355, Mar. 2018, doi: 10.1007/s40565-017-0332-x.
[32] S. Xia, K. W. Chan, X. Luo, S. Bu, Z. Ding, and B. Zhou, "Optimal sizing of energy storage system and its cost-benefit analysis for power grid planning with intermittent wind generation," *Renew. Energy*, vol. 122, pp. 472–486, Jul. 2018, doi: 10.1016/j.renene.2018.02.010.
[33] L. Bai, T. Jiang, F. Li, H. Chen, and X. Li, "Distributed energy storage planning in soft open point based active distribution networks incorporating network reconfiguration and DG reactive power capability," *Appl. Energy*, vol. 210, pp. 1082–1091, Jan. 2018, doi: 10.1016/j.apenergy.2017.07.004.
[34] M. Zidar, P. S. Georgilakis, N. D. Hatziargyriou, T. Capuder, and D. Škrlec, "Review of energy storage allocation in power distribution networks: Applications, methods and future research," *IET Generat., Transmiss. Distrib.*, vol. 10, no. 3, pp. 645–652, Mar. 2016, doi: 10.1049/iet-gtd.2015.0447.
[35] G. Carpinelli, F. Mottola, and D. Proto, "Probabilistic sizing of battery energy storage when time-of-use pricing is applied," *Electr. Power Syst. Res.*, vol. 141, pp. 73–83, Dec. 2016, doi: 10.1016/j.epsr.2016.07.013.
[36] G. Carpinelli, F. Mottola, and D. Proto, "Addressing technology uncertainties in battery energy storage sizing procedures," *Int. J. Emerg. Electr. Power Syst.*, vol. 18, no. 2, pp. 1–16, 2017, doi: 10.1515/ijeeps-2016-0199.
[37] G. J. Anders, *Probability Concepts in Electric Power Systems*. New York, NY, USA: Wiley, 1990.
[38] V. Miranda and L. M. Proenca, "Why risk analysis outperforms probabilistic choice as the effective decision support paradigm for power system planning," *IEEE Trans. Power Syst.*, vol. 13, no. 2, pp. 643–648, May 1998, doi: 10.1109/59.667394.
[39] E. Carpaneto, G. Chicco, P. Mancarella, and A. Russo, "Cogeneration planning under uncertainty. Part II: Decision theory-based assessment of planning alternatives," *Appl. Energy*, vol. 88, no. 4, pp. 1075–1083, Apr. 2011, doi: 10.1016/j.apenergy.2010.08.019.
[40] G. Carpinelli, A. R. di Fazio, S. Khormali, and F. Mottola, "Optimal sizing of battery storage systems for industrial applications when uncertainties exist," *Energies*, vol. 7, no. 1, pp. 130–149, 2014, doi: 10.3390/en7010130.
[41] G. Carpinelli, G. Celli, F. Pilo, and A. Russo, "Embedded generation planning under uncertainty including power quality issues," *Eur. Trans. Elect. Power*, vol. 13, no. 6, pp. 381–389, 2003, doi: 10.1002/etep.4450130607.
[42] C. Bordin, H. O. Anuta, A. Crossland, I. L. Gutierrez, C. J. Dent, and D. Vigo, "A linear programming approach for battery degradation analysis and optimization in offgrid power systems with solar energy integration," *Renew. Energy*, vol. 101, pp. 417–430, Feb. 2017, doi: 10.1016/j.renene.2016.08.066.
[43] B. Zhou, X. Liu, Y. Cao, C. Li, C. Y. Chung, and K. W. Chan, "Optimal scheduling of virtual power plant with battery degradation cost," *IET Gener., Transmiss. Distrib.*, vol. 10, no. 3, pp. 712–725, Feb. 2016, doi: 10.1049/iet-gtd.2015.0103.
[44] L. Lazard. (Nov. 2015). *Lazard's levelized Cost of Storage Analysis, Version 1.0*. [Online]. Available: https://www.lazard.com/media/2391/lazards-levelized-cost-of-storage-analysis-10.pdf
[45] O. Gandhi, C. D. Rodríguez-Gallegos, W. Zhang, D. Srinivasan, and T. Reindl, "Economic and technical analysis of reactive power provision from distributed energy resources in microgrids," *Appl. Energy*, vol. 210, pp. 827–841, Jan. 2018, doi: 10.1016/j.apenergy.2017.08.154.
[46] M. Braun, "Reactive power supplied by PV inverters-cost-benefit-analysis," in *Proc. 22nd Eur. Photovolt. Solar Energy Conf. Exhibit.*, Milan, Italy, Sep. 2007, pp. 1–7.
[47] A. Grace, *Optimization Toolbox User's Guide for Use With Matlab, Version 7.3*. Natick, MA, USA: MathWorks, Inc., 2015.
[48] S. P. Han, "A globally convergent method for nonlinear programming," *J. Optim. Theory Appl.*, vol. 22, no. 3, pp. 297–309, 1977, doi: 10.1007/BF00932858.
[49] A. Soroudi and T. Amraee, "Decision making under uncertainty in energy systems: State of the art," *Renew. Sustain. Energy Rev.*, vol. 28, pp. 376–384, Dec. 2013, doi: 10.1016/j.rser.2013.08.039.
[50] V. Miranda and L. M. Proenca, "Probabilistic choice vs. risk analysis-conflicts and synthesis in power system planning," *IEEE Trans. Power Syst.*, vol. 13, no. 3, pp. 1038–1043, Aug. 1998, doi: 10.1109/59.709095.
[51] *Benchmark Systems for Network Integration of Renewable and Distributed Energy Resources*, Cigré Task Force C6.04, Cigre Brochure 575, Paris, France, Apr. 2014.
[52] S. X. Chen, H. B. Gooi, and M. Q. Wang, "Sizing of energy storage for microgrids," *IEEE Trans. Smart Grid*, vol. 3, no. 1, pp. 142–151, Mar. 2012, doi: 10.1109/TSG.2011.2160745.
[53] International Renewable Energy Agency, Abu Dhabi, United Arab Emirates. (2017). *Electricity Storage and Renewables: Costs and Markets to 2030*. [Online]. Available: http://www.irena.org/publications/2017/Oct/Electricity-storage-and-renewables-costs-and-markets
[54] S. M. Schoenung and W. V. Hassenzahl, "Long- vs. short-term energy storage technologies analysis: A life-cycle cost study," Sandia Nat. Lab., Albuquerque, NM, USA, Sandia Rep. SAND2003-2783 2003. [Online]. Available: https://prod.sandia.gov/techlib-noauth/access-control.cgi/2003/032783.pdf
[55] M. A. Laughton, "Sensitivity in dynamical system analysis," *J. Electron. Control*, vol. 17, no. 5, pp. 577–591, 1964, doi: 10.1080/00207216408937730.
[56] M. A. Laughton and M. A. El-Iskandarani, "On the inherent network structure," in *Proc. 6th Power Syst. Comput. Conf.*, Darmstad, Germany, Nov. 1978, pp. 188–196.
[57] G. Carpinelli, A. Russo, M. Russo, and P. Verde, "Inherent structure theory of networks and power system harmonics," *IEE Proc.-Gener., Transmiss. Distrib.*, vol. 145, no. 2, pp. 123–132, Mar. 1998, doi: 10.1049/ip-gtd:19981663.
[58] G. M. Casolino and A. Losi, "Load Area model accuracy in distribution systems," *Electr. Power Syst. Res.*, vol. 143, pp. 321–328, Feb. 2017, doi: 10.1016/j.epsr.2016.10.044.

AMEDEO ANDREOTTI (M'97–SM'12) received the M.Sc. and Ph.D. degrees in electrical engineering from the University of Naples Federico II, Naples, Italy. He is currently an Associate Professor with the University of Naples Federico II. He is an Editor of technical journals in the field of power systems. His research interests include transients in power systems, lightning effects on power systems, electromagnetic compatibility, power quality, and smart grids. He is a member of the IEEE Working Group "Lightning Performance of Distribution Lines" and has been member of the section MT600 of the TC1 of the International Electrotechnical Commission.

GUIDO CARPINELLI (M'92) received the M.Sc. degree in electrical engineering from the University of Naples Federico II, Italy, in 1978. He is currently a Professor of energy electrical systems with the University of Naples Federico II. He has authored several papers in journals published by the IEEE, IEE, IET, and Elsevier. He has published a book on power quality indices edited by J. Wiley and co-authored several book chapters. His research interest concerns power quality and power system analysis. He participates in the IEEE and CIGRE working groups on power quality.

FABIO MOTTOLA (M'07–SM'18) received the M.Sc. and Ph.D. degrees in electrical engineering from the University of Naples Federico II, Naples, Italy, in 2004 and 2008, respectively. His research interests include the planning and operation of electrical power systems in the presence of distributed energy resources and lightning effects on power systems.

DANIELA PROTO (M'09–SM'17) received the M.Sc. and Ph.D. degrees in electrical engineering from the University of Naples Federico II, Naples, in 2000 and 2004, respectively, and the postgraduate master's degree in software technologies from the University of Sannio, Benevento, Italy, in 2001. She is currently an Assistant Professor with the University of Naples Federico II. Her research interests include electrical power systems and electrical transport systems.

ANGELA RUSSO (M'16–SM'18) received the M.Sc. degree in electrical engineering and the Ph.D. degree in industrial engineering from the Università degli Studi di Cassino, Cassino, Italy, in 1996 and 2000, respectively. She is currently an Associate Professor of electrical power systems with the Energy Department, Politecnico di Torino, Turin, Italy. Her research interest concerns power quality and power system analysis.